Dalton Transactions

Accepted Manuscript

This article can be cited before page numbers have been issued, to do this please use: X. Sun, J. Dong, Z. Li, H. Liu, X. Jing, Y. Chi and C. Hu, *Dalton Trans.*, 2019, DOI: 10.1039/C9DT00395A.

This is an Accepted Manuscript, which has been through the Royal Society of Chemistry peer review process and has been accepted for publication.

Accepted Manuscripts are published online shortly after acceptance, before technical editing, formatting and proof reading. Using this free service, authors can make their results available to the community, in citable form, before we publish the edited article. We will replace this Accepted Manuscript with the edited and formatted Advance Article as soon as it is available.

You can find more information about Accepted Manuscripts in the author guidelines.

Please note that technical editing may introduce minor changes to the text and/or graphics, which may alter content. The journal's standard Terms & Conditions and the ethical guidelines, outlined in our author and reviewer resource centre, still apply. In no event shall the Royal Society of Chemistry be held responsible for any errors or omissions in this Accepted Manuscript or any consequences arising from the use of any information it contains.

ROYAL SOCIETY OF CHEMISTRY

rsc.li/dalton

View Article Online
DOI: 10.1039/C9DT00395A

ARTICLE

Mono-Transition-Metal-Substituted Polyoxometalate Intercalated Layered Double Hydroxides for the Catalytic Decontamination of Sulfur Mustard Simulant

Received 00th January 20xx,
Accepted 00th January 20xx

DOI: 10.1039/x0xx00000x

Xiangrong Sun, Jing Dong, Zhen Li, Huifang Liu, Xiaoting Jing, Yingnan Chi*, Changwen Hu

The Keggin-type mono-transition-metal-substituted $[PW_{11}M(H_2O)O_{39}]^{5-}$ ($PW_{11}M$, M = Ni, Co, Cu) were intercalated into Zn_2Cr-based layered double hydroxide (Zn_2Cr-LDH) by an exfoliation-reassembly method and the synthesized Zn_2Cr-LDH-$PW_{11}M$ composites were thoroughly characterized by Fourier transform infrared (FT-IR), powder X-ray diffraction (PXRD), solid state ^{31}P nuclear magnetic resonance (^{31}P NMR), thermogravimetric analysis (TGA), inductively coupled plasma atomic emission spectroscopy (ICP-AES), scanning electron microscopy (SEM) and transmission electron microscopy (TEM). The three composites can be used as heterogeneous catalysts to promote the oxidative decontamination of the sulfur mustard simulant, 2-chloroethyl ethyl sulfide (CEES). Interestingly, a cooperative effect between $PW_{11}M$ cluster and Zn_2Cr-LDH is evidenced by the fact that the composites have a higher catalytic performance than either of the individual constituents alone. The catalytic activity of Zn_2Cr-LDH-$PW_{11}M$ is significantly influenced by the substituted transition metals, showing the order: Zn_2Cr-LDH-$PW_{11}Ni$ > Zn_2Cr-LDH-$PW_{11}Co$ > Zn_2Cr-LDH-$PW_{11}Cu$. Under the ambient conditions, Zn_2Cr-LDH-$PW_{11}Ni$ composite can convert 98% of CEES in 3 h using nearly stoichiometric 3% aqueous H_2O_2 with the selectivity of 94% for nontoxic product, 2-chloroethyl ethyl sulfoxide (CEESO). Moreover, the decontaminating material, Zn_2Cr-LDH-$PW_{11}Ni$, is stable to leaching and can be readily reused for up to ten cycles without obvious lose of its activity.

Introduction

Bis(2-chloroethyl) sulfide, commonly called sulfur mustard or HD, is a powerful vesicant that can directly damage tissue cells, cause local inflammation, and lead to systemic poisoning even death in high doses.[1] Since it was first used effectively in World War I, sulfur mustard becomes the most produced, stored and used chemical warfare agent (once known as the "King of the Battle Gases").[2] Although an international treaty prohibiting the production and use of sulfur mustard has been signed in 1992, this compound was still repeatedly used in recent terrorist attacks. In general, sulfur mustard can be neutralized by three pathways: oxidation[3-7], dehydrohalogenation[8-10], and hydrolysis[11-14] (Scheme 1). However, the slow degradation rate of dehydrochlorination and hydrolysis limits their practical application. In comparison, the selective oxidation is a highly attractive way, especially using molecular oxygen or hydrogen peroxide as oxidant. During the decontamination, the selectivity is very important because the partially oxidation product, sulfoxide, is less toxic but the over-oxidation product, sulfone, is still as toxic as sulfur mustard. Until now, several kinds of catalysts for sulfur mustard degradation have been studied including metal oxides[15-18], polyoxometalates (POMs)[6, 7, 19], and coordination polymers[20-22].

Scheme 1. The three decontamination pathways of sulfur mustard.

POMs are a family of discrete polyanionic clusters, which are mainly composed of Mo, W, V, Nb centers and oxo ligands.[23, 24] Owing to their excellent multi-electron redox property, POMs can effectively catalyze a series of oxidation reactions.[25-29] The investigations in Hill's group indicate that transition metal containing POMs, such as $\{PV_2Mo_{10}O_{40}\}$[30-35], $\{FePW_{11}O_{39}\}$[36], $\{(Fe^{III}(OH_2)_2)_3(PW_9O_{34})_2\}$[37, 38], and $\{(FeOH_2)_2Fe_2(P_2W_{15}O_{56})_2\}$[39] are active catalysts for the oxidative decontamination of sulfur mustard and its simulants. Since POMs have high solubility in water and other polar solvents, the reusability of them after catalysis remains a great challenge. From the practical point of view, the development of personal protective equipment needs materials that not only can catalytically decompose sulfur mustard but also can be integrated into suits, gloves, and

Key Laboratory of Cluster Science Ministry of Education, Beijing Key Laboratory of Photoelectronic/Electrophotonic Conversion Materials, School of Chemistry and Chemical Engineering
Beijing Institute of Technology
Beijing, 100081 (P.R. China)
E-mail: chiyingnan7887@bit.edu.cn
† Footnotes relating to the title and/or authors should appear here.
Electronic Supplementary Information (ESI) available: [details of any supplementary information available should be included here]. See DOI: 10.1039/x0xx00000x

View Article Online
DOI: 10.1039/C9DT00595A

boots.[40] Therefore, several POM-based decontamination materials were synthesized by immobilizing POMs on carbon[33, 41], fibers[30, 32, 42], metal organic frameworks (MOFs) [35, 43], or nanoparticles[44-46].

Layered double hydroxides (LDHs) are assembled from positively charged layers and interlayer anions by electrostatic and hydrogen bonding interactions.[47] The good interlayer anion-exchange ability and the tunable charge density and acid/base property make LDH an excellent host to immobilize POMs. The first reported LDH-POM material is Zn_2Al-LDH-$V_{10}O_{28}$, which shows enhanced photocatalytic activity in the oxidation of isopropanol.[48] Subsequently, a series of LDH-POM materials have been prepared and used in catalytic transformations of thiophene oxidation [49, 50], olefin epoxidation[51-54], esterification[55-57], and so on. Although POMs inserted LDH materials have been proven to be active for the oxidation of sulfides in the presence of H_2O_2 by Song et al, [58-60] such kind of material is rarely used in the oxidative decontamination of chemical warfare agents or their simulants.[61]

In this work, three decontaminating composites, Zn_2Cr-LDH-$PW_{11}M(H_2O)O_{39}$ (for **1**, M = Ni; for **2**, M = Co; for **3**, M = Cu) have been successfully prepared by intercalating mono-transition-metal-substituted Keggin-type tungstophosphate into Zn_2Cr-LDH-NO_3 and thoroughly characterized by Fourier transform infrared (FT-IR), powder X-ray diffraction (PXRD), solid state ^{31}P nuclear magnetic resonance (^{31}P NMR), thermogravimetric analysis (TGA), inductively coupled plasma atomic emission spectroscopy (ICP-AES) and Brunauer-Emmett-Teller (BET). The three composites can catalyze the selective oxidation of sufur mustard simulant, 2-chloroethyl ethyl sulfide (CEES), in the presence of nearly stoichiometric 3% hydrogen peroxide and the catalytic performance of **1** is better than those of **2** and **3**. Using **1** as heterogeneous catalyst, 98% CEES was converted in 3 h with 94% selectivity under ambient conditions. The Zn_2Cr-LDH-$PW_{11}Ni$ (**1**) is robustness and can be reused for ten cycles without significant loss of its activity.

Experimental

Materials and methods

$H_3PW_{12}O_{40}$ and the nitrate salts of Ni, Co, Cu, Zn, Cr were purchased from Sinopharm Chemical Reagent Co., Ltd.. NaOH, KCl, Li_2CO_3, aqueous H_2O_2, and CEES were purchased from Aladdin Industrial Corporation. **CAUTION:** The simulant of HD, CEES, is highly toxic and the decontamination experiments should be performed carefully by the trained personnel in a hood under good ventilation. PXRD data were collected on a Bruker instrument (D8 Venture) equipped with graphite-monochromatized Cu Kα radiation (λ = 0.154 nm; scan speed = 5° min^{-1}; 2θ = 5-70°) at room temperature. The FT-IR spectra were measured on a Nicolet 170SXFT-IR spectrophotometer in the range 400-4000 cm^{-1}. The elemental analyses of Zn, Cr and W were performed by a ThermoiCAP 6000 atomic emission spectrometer. Thermogravimetric data were collected on a Shimadzu DTG-60AH thermal analyzer under air atmosphere with a heating rate of 10 °C min^{-1}. Scanning electron microscopy (SEM, JOEL JSE-7500F) and transmission electron microscopy (TEM, JOEL JEM-2010) were used to observe the morphology and microstructure of the samples. The BET specific surface areas were measured at 77 K by using a Belsorp-max surface area detecting instrument. The X-ray photoelectron spectroscopy (XPS) W4f spectrum was performed on ESCALAB 250Xi. Solid state ^{31}P NMR were performed at room temperature on 700 MHz Bruker Ascend spectrometer. The degradation of CEES was monitored by gas chromatograph (Shimadzu GC-2014C) equipped with a flame ionization detector (FID) and a HP-5 ms capillary column.

Synthesis of Zn_2Cr-LDH-$PW_{11}M(H_2O)O_{39}$ Composites

Synthesis of $K_5PW_{11}M(H_2O)O_{39}$ (M = Ni^{II}, Co^{II}, and Cu^{II}). $K_5PW_{11}M(H_2O)O_{39}$ (M = Ni^{II}, Co^{II}, and Cu^{II}) were prepared according to the reported methods.[62] $H_3PW_{12}O_{40}$ were dissolved in deionized water (80 °C) and the pH of the solution was adjusted to 4.8 by adding Li_2CO_3 solution. To this, the nitrate salts of Ni, Co, or Cu and KCl powder were added and the mixture was filtered while hot. The filtrates were placed in a refrigerator overnight and then crystals were observed and collected. The crystals were dissolved in a small amount of hot water for recrystallization.

Synthesis of Zn_2Cr-LDH-NO_3. The Zn_2Cr-LDH-NO_3 was synthesized according to literature by the conventional co-precipitation method.[63] A 20 mL solution containing 0.66 M of $Zn(NO_3)_2$ and 0.33 M of $Cr(NO_3)_3$ and 50 mL NaOH (2M) were simultaneously dropped into a 150 mL boiled deionized water with vigorous stirring under N_2 atmosphere and the final pH of the solution was controlled to about 5.5. After aging at 80 °C for 12 h, the light purple precipitate (Zn_2Cr-LDH-NO_3) was filtered and washed by deionized water and ethanol, respectively, and dried at 60 °C for 12 h.

Synthesis of Zn_2Cr-LDH-$PW_{11}M$ composites. In order to obtain exfoliated Zn_2Cr-LDH nanosheets, the prepared Zn_2Cr-LDH-NO_3 was dispersed into 20 mL formamide to form a colloidal suspension.[63] To this, the aqueous solution of $K_5PW_{11}M(H_2O)O_{39}$ was added dropwise and the mixture was stirred for 30 min under ambient conditions. The crude product was washed with water and ethanol, respectively, and dried under vacuum at 80 °C for 12 h.

Catalytic oxidation of CEES.

The selective oxidation (decontamination) of CEES using different catalysts were carried out as follows. Catalyst (0.0015 mmol) was dispersed in acetonitrile (4 mL), followed by addition of CEES (0.5 mmol) and 1,3-dichlorobenzene (internal standard, 0.25 mmol). After stirring for 2 minutes at room temperature, 3% aqueous H_2O_2 (0.525 mmol) was added dropwise. The reaction was monitored by gas chromatography at various time intervals and the products were qualitatively analyzed by GC-MS. In the recycle experiments, the catalyst **1** was filtered after the reaction and washed with ethyl acetate and dried under vacuum at 50 °C and used for the next cycle.

View Article Online
DOI: 10.1039/C9DT00795A

Results and discussion

Synthesis and Characterization of Zn_2Cr-LDH-$PW_{11}M$.

As transition metal containing POMs have been proven to be active in the selective oxidation of sulfur mustard and/or its simulants, in our experiment three mono-transition-metal-substituted Keggin-type $PW_{11}M$ (M = Ni^{II}, Co^{II}, and Cu^{II}) were used to combine with LDH. Zn_2Cr-LDH-NO_3 was chosen as the host based on the following considerations. First, Zn_2Cr-LDH-NO_3 is formed under weak acidic conditions, which is more compatible with the working pH range of polyanion $PW_{11}M$ than other basic LDH, such as Mg_2Al-LDH-NO_3 and Zn_2Al-LDH-NO_3. Second, we found that the activity of Zn_2Cr-LDH-NO_3 host as heterogeneous catalysts is better than those of Zn_2Al-LDH-NO_3 and Mg_2Al-LDH-NO_3 in the oxidation of CEES (Table 1, entry 9-11). As shown in Scheme 2, Zn_2Cr-LDH-$PW_{11}M$ was prepared by an exfoliation-reassembly method. The Zn_2Cr-LDH-NO_3 was first synthesized by the co-precipitation of $Zn(NO_3)_2$ and $Cr(NO_3)_3$ solution with NaOH under N_2 atmosphere. After aging at 80 °C for 12 h, the resulting precipitate was washed with deionized water and dried at 60 °C. The Zn_2Cr-LDH-NO_3 was exfoliated by formamide to form colloidal nanosheet suspension and to this $PW_{11}M$ solution was added dropwise. After 30 min stirring, Zn_2Cr-LDH-$PW_{11}M$ composite was obtained.

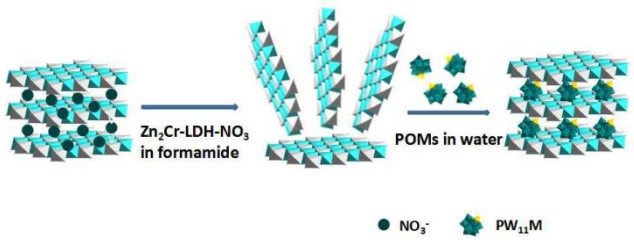

Scheme 2. The synthesis process of Zn_2Cr-LDH-$PW_{11}M$ by an exfoliation-reassembly method.

The PXRD patterns of three synthesized composites and Zn_2Cr-LDH-NO_3 are shown in Figure 1a. For LDH, the (003) diffraction peak is related to the layer spacing. When small nitrate is replaced by large $PW_{11}M$, the spacing layers are enlarged and the (003) peak correspondingly shifts to lower position. For three Zn_2Cr-LDH-$PW_{11}M$ composites, the characteristic (003) diffraction peaks obviously shift left compared with that of LDH host indicating the successful intercalation of POMs. According to the basal spacing of *d*(003), the gallery height value of 1.06 nm is calculated, which is in good accordance with the diameter of Keggin-type cluster. In addition, the (110) diffraction peaks (2θ = ~60°) and a broad hump diffraction peaks (2θ = ~32-42°) are nearly unchanged revealing that the layered structure of LDH is maintained after the intercalation of $PW_{11}M$.

The FT-IR spectra of composite **1**, LDH host, and POM precursor are shown in Figure 1b. The three mono-substituted $PW_{11}M$ exhibit similar characteristic peaks (Figure S1) at about 1080， 940， 880， 807 cm^{-1}, which are attributed to the vibrations of the P-O_a (a: tetrahedral oxygen atoms), W-O_d (d: terminal oxygen atoms), W-O_b-W (b: corner-shared oxygen atoms) and W-O_c (c: edge-shared oxygen atoms), respectively. The Zn_2Cr-LDH-NO_3 host shows a strong peak at 1385 cm^{-1} due to the vibration of NO_3^- anion. Compared with LDH host and POM precursors, the synthesized three composites have all the characteristic peaks of mono-substituted POMs but the absorption band of NO_3^- anion is much weaker. The FT-IR spectra further confirms successful intercalation of $PW_{11}M$ into Zn_2Cr-LDH. Compared with POM precursors, the characteristic absorption bands of POMs in Zn_2Cr-LDH-$PW_{11}M$ are slightly redshifted, which might be caused by the electrostatic and hydrogen bonding interactions between polyanions and the host.

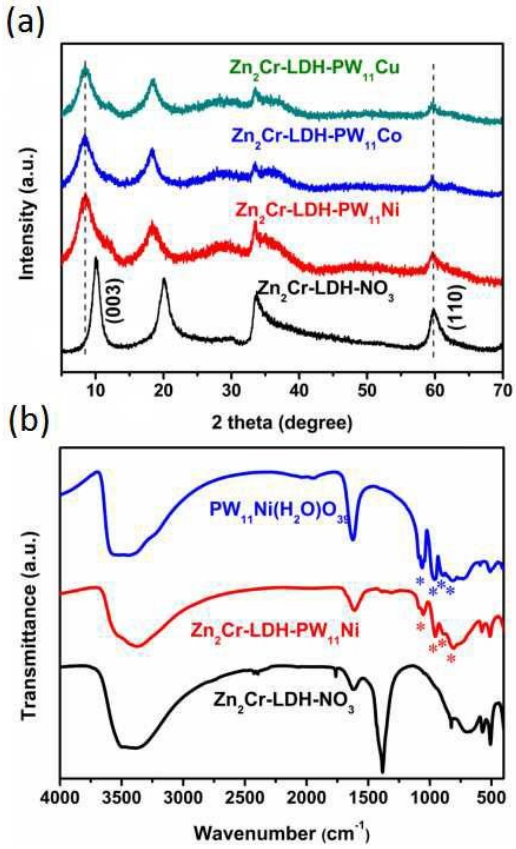

Figure 1. (a) The PXRD patterns of Zn_2Cr-LDH-$PW_{11}M$ and Zn_2Cr-LDH-NO_3; (b) FT-IR spectra of Zn_2Cr-LDH--NO_3, Zn_2Cr-LDH-$PW_{11}Ni$, and $PW_{11}Ni$.

The Zn_2Cr-LDH-$PW_{11}Ni$, composite **1**, was selected as a representative example for the following characterizations. Based on the SEM and TEM images (Figure 2a-2c), we found that Zn_2Cr-LDH-$PW_{11}Ni$ still has a typical LDH nanosheet morphology and compared with the image of Zn_2Cr-LDH-NO_3 no structure change is observed. Energy dispersive X-ray spectroscopy (EDS) (Figure S2) indicates that composite **1** contains Zn, Cr, P, W, Ni, and O elements and the tungsten and nickel are evenly dispersed on the LDH layers, that is proven by elemental mapping measurements (Figure 2d). The ICP-AES analyses indicate that the loading amount of $PW_{11}Ni$ is 52 wt%

View Article Online
DOI: 10.1039/C9DT00395A

corresponding to 60% exchange rate of NO_3^-. The XPS W4f spectrum of Zn_2Cr-LDH-$PW_{11}Ni$ is shown in Figure S3, where two well-resolved peaks at 37.7 and 35.6 eV correspond to $W4f_{5/2}$ and $W4f_{7/2}$, respectively.

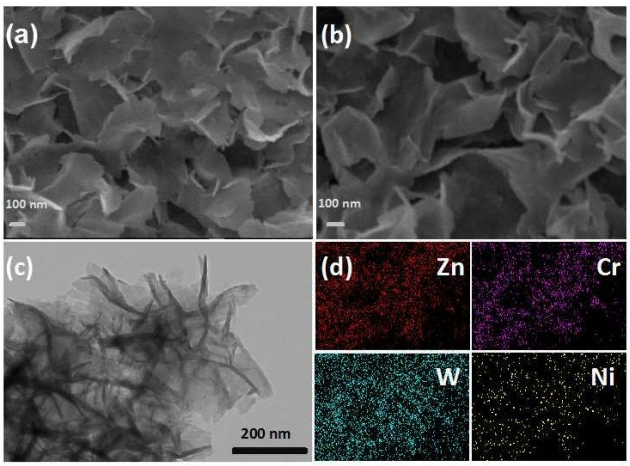

Figure 2. (a) SEM image of Zn_2Cr-LDH-NO_3; (b) SEM image of Zn_2Cr-LDH-$PW_{11}Ni$; (c) TEM image of Zn_2Cr-LDH-$PW_{11}Ni$; (d) Elemental mapping of Zn_2Cr-LDH-$PW_{11}Ni$.

Solid state ^{31}P NMR of composite **1** (Figure 3a) shows that the characteristic peak of $PW_{11}Ni$ at δ = -11.3 ppm still can be found in the Zn_2Cr-LDH-$PW_{11}Ni$. In addition, the N_2 adsorption-desorption isotherms of **1** were measured to assess its porosity. As shown in Figure 3b, composite **1** exhibits the type IV isotherm pattern with a clear hysteresis loop indicating the presence of mesopores. Composite **1** has a BET surface area of 24.92 m^2/g, which is higher than that of LDH host (13.56 m^2/g) and average pore size of the composite (42.48 nm) is also larger than that of host (14.14 nm). The results display that the intercalation of POM leads to the increase of surface area and the increased surface area might not only facilitates the exposure of catalyst active sites (POMs), but also contribute to the improvement of catalytic activity.

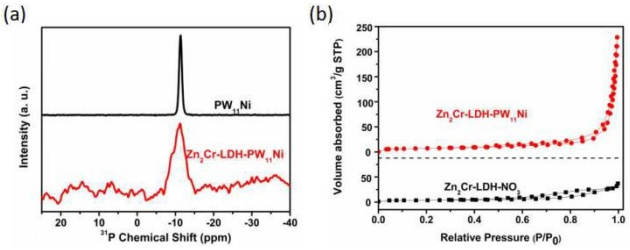

Figure 3. (a) Solid state ^{31}P NMR spectra of Zn_2Cr-LDH-NO_3 and Zn_2Cr-LDH-$PW_{11}Ni$; (b) The N_2 adsorption-desorption isotherms of Zn_2Cr-LDH-$PW_{11}Ni$.

Decontamination of CEES

The catalytic performance of three Zn_2Cr-LDH-$PW_{11}M$ composites **1-3** was evaluated in the oxidative decontamination of CEES, which is a widely used simulant for sulfur mustard. In a typical degradation reaction, CEES (0.5 mmol), 1,3-dichlorobenzene (internal standard, 0.25 mmol) and catalyst (0.0015 mmol) were mixed in acetonitrile (4 mL) and stirred for 2 min under ambient conditions, and then 3 % aqueous H_2O_2 (0.525 mmol) was added to initiate the reaction. As shown in Figure 4b and Table 1, entry 1-3, all the composites as heterogeneous catalysts can promote the oxidation of CEES and 76-98% CEES is converted in 3 h. The catalytic activity of composite **1** with the conversion of 98% is better than that of **2** (91%) or **3** (76%). In comparison, a negligible conversion of CEES is provided in the blank experiment (without catalysts). In the oxidation of CEES, the selectivity is an important parameter to be considered. The partial oxidation product, nontoxic 2-chloroethyl ethyl sulfoxide (CEESO), is more preferred than the over oxidation product, toxic 2-chloroethyl ethyl sulfone ($CEESO_2$). In our case, very similar selectivity (94%) for CEESO is given by three composites (Figure 4b and Table 1, entry 1-3).

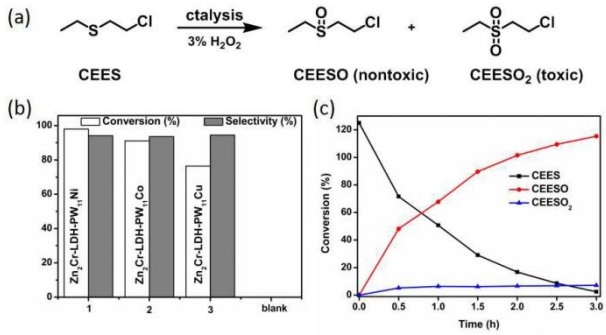

Figure 4. (a) Catalytic decontamination of CEES; (b) CEES oxidation using different Zn_2Cr-LDH-$PW_{11}M$ composites; (c) Time profile for CEES oxidative transformation using Zn_2Cr-LDH-$PW_{11}Ni$. Reaction conditions: Catalyst (0.0015 mmol), CEES (0.5 mmol), and 1,3-dichlorobenzene (0.25 mmol), 3% aqueous H_2O_2 (0.525 mmol) and acetonitrile (4 mL) at room temperature.

To probe the role of two components: $PW_{11}M$ and Zn_2Cr-LDH in the degradation of CEES, a series of control experiments were conducted (Table 1). First, the potassium salts of $PW_{11}M$ were used and they can decontaminate CEES in homogeneous system with the conversion of 81% for $PW_{11}Ni$, 78% for $PW_{11}Co$, and 73% for $PW_{11}Cu$, respectively (Table 1, entry 4-6). Under otherwise identical conditions, the host, Zn_2Cr-LDH, only converts 30% of CEES, which is far lower than that of $PW_{11}M$ (73-81%). The above results indicate that in the Zn_2Cr-LDH-$PW_{11}M$ composites the inserted POM clusters are the main catalytic active sites. More importantly the cooperative effect between $PW_{11}M$ and Zn_2Cr-LDH is evident because the composites have a higher catalytic performance than either of the individual constituents alone. To assess the influence of substituted transition metals on the decontamination process, plenary $H_3PW_{12}O_{40}$ and lacunary $K_7PW_{11}O_{39}$ were used (Table 1, entry 7-8). Under the same conditions, the conversions of $H_3PW_{12}O_{40}$ (21%) and $K_7PW_{11}O_{39}$ (58%) are lower than those of $PW_{11}M$ (73-81%), indicating that both the tungstophosphate and the substituted transition metals contribute to the catalytic decontamination. It is interesting to note that the order of catalytic activity for Zn_2Cr-LDH-$PW_{11}M$ composites (**1** > **2** > **3**) is

View Article Online
DOI: 10.1039/C9DT00325A

consistent with that observed in homogeneous system ($PW_{11}Ni$ > $PW_{11}Co$ > $PW_{11}Cu$) and that further confirms the important role of substituted transition metals in the oxidation of CEES. As the good performance, composite **1** with TON of 327 was used in the following experiments. To explore the influence of catalyst or oxidant on the degradation of CEES, the catalytic reactions with different amount of catalyst or oxidant were performed. We find that the conversion of CEES increases with the dosage of composite **1** or oxidant (Figure S6).

Table 1. Decontamination of CEES using different catalysts

Entry	Catalyst	System	Conversion (%)	Selectivity (%)
1	Zn_2Cr-LDH-$PW_{11}Ni$	Heterogeneous	98	94
2	Zn_2Cr-LDH-$PW_{11}Co$	Heterogeneous	91	93
3	Zn_2Cr-LDH-$PW_{11}Cu$	Heterogeneous	76	94
4	$K_5PW_{11}Ni(H_2O)O_{39}$	Homogeneous	81	93
5	$K_5PW_{11}Co(H_2O)O_{39}$	Homogeneous	78	89
6	$K_5PW_{11}Cu(H_2O)O_{39}$	Homogeneous	73	90
7	$K_7PW_{11}O_{39}$	Homogeneous	58	92
8	$H_3PW_{12}O_{40}$	Homogeneous	21	91
9	Mg_2Al-LDH-NO_3	Heterogeneous	<10	99
10	Zn_2Al-LDH-NO_3	Heterogeneous	<10	99
11	Zn_2Cr-LDH-NO_3	Heterogeneous	30	96

Reaction conditions: Catalyst (0.0015 mmol), CEES (0.5 mmol), and 1,3-dichlorobenzene (0.25 mmol), 3% aqueous H_2O_2 (0.525 mmol) and acetonitrile (4 mL) at room temperature.

The degradation profile for Zn_2Cr-LDH-$PW_{11}Ni$, composite **1**, is shown in Figure 4c, where about 50% of CEES is converted in 40 min. The undesired product, toxic $CEESO_2$, is formed in the first 30 min but during the following 2.5 h its amount is nearly unchanged even though the concentration of CEESO is greatly increased. This is different from the phenomenon reported in niobium saponite clay, where the selectivity for CEESO is dramatically decreased when the conversion of CEES reached maximum.[3] Compared with the reported catalytic materials, Zn_2Cr-LDH-$PW_{11}Ni$ composite has the following two advantages: 1) exhibiting a higher selectivity for nontoxic CEESO (94%); 2) using green dilute H_2O_2 (3%) as oxidant. For example, niobium saponite clay gave a selectivity of 71% by using 5 equiv. 30% H_2O_2 and PW_{12}@NU-1000 formed by incorporating $H_3PW_{12}O_{40}$ into MOF has a selectivity of 57% in the presence of 1.5 equiv. 30% H_2O_2, and $H_5PV_2Mo_{10}O_{40}$ supported on porous carbon materials oxidize sulfur mustard simulant by *tert*-butylhydroperoxide.[3, 32, 43] In addition, the efficiency of H_2O_2 utilization in the composite **1** system is as high as 98.9%.

A leaching test was performed to check the heterogeneous nature of Zn_2Cr-LDH-$PW_{11}Ni$. When the reaction was carried out for 0.5 h with the conversion of about 43%, the catalyst was filtered off and the filtrate continued to react under the same conditions for 2.5 h giving a negligible conversion of CEES (Figure 5a). The result displays that the synthesized catalytic material is stable to leaching under turnover conditions and Zn_2Cr-LDH is an efficient host to immobilize $PW_{11}Ni$. Moreover, the recyclability and stability of composite **1** were evaluated. As shown in Figure 5b, after 10 cycles only a slight decrease in conversion and selectivity was found. In addition, the comparison of FT-IR and PXRD spectra before and after the recycle test confirms that the structure of Zn_2Cr-LDH-$PW_{11}Ni$ is maintained during the recycle (Figure S7).

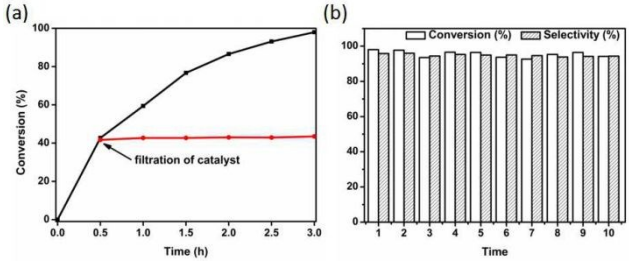

Figure 5. (a) Leaching test for CEES decontamination using Zn_2Cr-LDH-$PW_{11}Ni$; (b) Recycle test for CEES decontamination using Zn_2Cr-LDH-$PW_{11}Ni$. Reaction conditions: Catalyst (0.0015 mmol), CEES (0.5 mmol), and 1,3-dichlorobenzene (0.25 mmol), 3% aqueous H_2O_2 (0.525 mmol) and acetonitrile (4 mL) at room temperature.

For the oxidation reaction with hydrogen peroxide as oxidant, both radical and nonradical processes could be involved. To reveal the mechanism of the reaction, several radical scavengers including *p*-benzoquinone for $\bullet O_2^-/\bullet O_2H$ and *tert*-butyl alcohol and diphenylamine for $\bullet OH$ were used in the oxidative detoxification of CEES. As shown in Table S1, the conversion of CEES is nearly unchanged after adding radical scavengers, indicating that it's not a radical reaction process. Therefore, we proposed a possible nonradical mechanism: hydrogen peroxide is activate by the intercalated $PW_{11}M$ cluster to form active peroxo-species, which subsequently oxidize CEES to CEESO. Our speculation is supported by previous investigations that both the polyoxotungstates and the substituted transition metals on POMs can react with hydrogen peroxide to form active peroxo-species.[64-66]

Conclusions

In summary, three novel decontaminating composites, Zn_2Cr-LDH-$PW_{11}M$ (M = Ni, Co, Cu), were successfully fabricated by intercalating Keggin-type $PW_{11}M$ into Zn_2Cr-LDH host and thoroughly characterized by routine techniques. In the oxidative degradation of CEES (a sulfur mustard simulant), Zn_2Cr-LDH-$PW_{11}Ni$ exhibits a better catalytic performance (conversion: 98%, selectivity: 94%) than other two counterparts. Notably, Zn_2Cr-LDH not only acts as an excellent host for the stable immobilization of $PW_{11}M$ polyanions but also contributes to the enhancement of catalytic activity. The Zn_2Cr-LDH-$PW_{11}Ni$ with stable structure and good recyclability is a promising catalytic material for the effective decontamination of sulfur mustard and has potential application in the fabrication of personal protective equipment.

Conflicts of interest

There are no conflicts to declare.

Acknowledgements

This work was financially supported by the National Natural Science Foundation of China (21671019, 21871026, 21771020), 973 Program (2014CB932103).

Notes and references

1 K. Kehe and L. Szinicz, *Toxicology*, 2005, **214**, 198-209.
2 M. J. Geraci, *Ann Pharmacother*, 2008, **42**, 237-246.
3 F. Carniato, C. Bisio, R. Psaro, L. Marchese and M. Guidotti, *Angew Chem Int Ed*, 2014, **53**, 10095-10098.
4 E. L. Clennan, W. H. Zhou and J. Chan, *J Org Chem*, 2002, **67**, 9368-9378.
5 A. J. Howarth, C. T. Buru, Y. Liu, A. M. Ploskonka, K. J. Hartlieb, M. McEntee, J. J. Mahle, J. H. Buchanan, E. M. Durke, S. S. Al-Juaid, J. F. Stoddart, J. B. DeCoste, J. T. Hupp and O. K. Farha, *Chem Eur J*, 2017, **23**, 214-218.
6 J. Dong, J. F. Hu, Y. N. Chi, Z. G. Lin, B. Zou, S. Yang, C. L. Hill and C. W. Hu, *Angew Chem*, 2017, **129**, 1-6.
7 X. Li, J. Dong, H. Liu, X. Sun, Y. Chi and C. Hu, *J Hazard Mater*, 2018, **344**, 994-999.
8 G. W. Wagner, P. W. Bartram, O. Koper and K. J. Klabunde, *J Phys Chem B*, 1999, **103**, 3225-3228.
9 D. A. Giannakoudakis, J. K. Mitchell and T. J. Bandosz, *J Mater Chem A*, 2016, **4**, 1008-1019.
10 A. Saxena, A. K. Srivastava, A. Sharma and B. Singh, *J Hazard Mater*, 2009, **169**, 419-427.
11 G. K. Prasad, T. H. Mahato, B. Singh, K. Ganesan, P. Pandey and K. Sekhar, *J Hazard Mater*, 2007, **149**, 460-464.
12 A. Roy, A. K. Srivastava, B. Singh, T. H. Mahato, D. Shah and A. K. Halve, *Micropor Mesopor Mater*, 2012, **162**, 207-212.
13 S. Y. Bae and M. D. Winemiller, *J Org Chem*, 2013, **78**, 6457-6470.
14 B. Sigh, T. H. Mahato, A. K. Srivastava, G. K. Prasad, K. Ganesan, R. Vijayarghavan and R. Jain, 2011, *J Hazard Mater*, 2007, **190**, 1053-1057.
15 G. W. Wagner, O. B. Koper, E. Lucas, S. Decker and K. J. Klabunde, *J. Phys. Chem. B,* 2000, **104**, 5118-5123.
16 G. W. Wagner, G. W. Peterson and J. J. Mahle, *Ind Eng Chem Res*, 2012, **51**, 3598-3603.
17 C. Bisio, F. Carniato, C. Palumbo, S. L. Safronyuk, M. F. Starodub, A. M. Katsev, L. Marchese and M. Guidotti, *Catal Today*, 2016, **277**, 192-199.
18 K. F. Cheng, F. C. Yang, K. H. Wu and X. M. Liu, *Mater Sci Eng C*, 2018, **93**, 615-622.
19 Y. J. Hou, H. Y. An, Y. M. Zhang, T. Hu, W. Yang and S. Z. Chang, *ACS Catal*, 2018, **8**, 6062-6069.
20 Y. Y. Liu, S. Y. Moon, J. T. Hupp and O. K. Farha, *Acs Nano*, 2015, **9**, 12358-12364.
21 E. Lopez-Maya, C. Montoro, L. M. Rodriguez-Albelo, S. D. A. Cervantes, A. A. Lozano-Perez, J. L. Cenis, E. Barea and J. A. R. Navarro, *Angew Chem Int Ed*, 2015, **54**, 6790-6794.
22 W. Q. Zhang, K. Cheng, H. Zhang, Q. Y. Li, Z. Ma, Z. Wang, J. Sheng, Y. Li, X. Zhao and X. J. Wang, *Inorg Chem*, 2018, **57**, 4230-4233.
23 Y. P. Jeannin, *Chem Rev*, 1998, **98**, 51-76.
24 D. L. Long, R. Tsunashima and L. Cronin, *Angew Chem Int Ed*, 2010, **49**, 1736-1758.
25 C. L. Hill, *in Chem Rev*, Vol. 98, No. 1, 1998, pp. 1-390.
26 O. A. Kholdeeva, N. V. Maksimchuk and G. M. Maksimov, *Catal Today*, 2010, **157**, 107-113.
27 N. Mizuno, K. Kamata and K. Yamaguchi, *Top Catal*, 2010, **53**, 876-893.
28 H. N. Miras, J. Yan, D. L. Long and L. Cronin, *Chem Soc Rev*, 2012, **41**, 7403-7430.
29 H. J. Lv, Y. V. Geletii, C. C. Zhao, J. W. Vickers, G. B. Zhu, Z. Luo, J. Song, T. Lian, D. G. Musaev and C. L. Hill, *Chem Soc Rev*, 2012, **41**, 7572-7589.
30 L. Xu, E. Boring and C. L. Hill, *J Catal*, 2000, **195**, 394-405.
31 R. D. Gall, M. Faraj and C. L. Hill, *Inorg Chem*, 1994, **33**, 5015-5021.
32 R. D. Gall, C. L. Hill and J. E. Walker, *Chem Mater*, 1996, **8**, 2523-2527.
33 R. D. Gall, C. L. Hill and J. E. Walker, *J Catal*, 1996, **159**, 473-478.
34 N. M. Okun, T. M. Anderson, K. I. Hardcastle and C. L. Hill, *Inorg Chem*, 2003, **42**, 6610-6612.
35 Y. Q. Li, Q. Gao, L. J. Zhang, Y. S. Zhou, Y. X. Zhong, Y. Ying, M. C. Zhang, C. Q. Huang and Y. A. Wang, *Dalton Trans*, 2018, **47**, 6394-6403.
36 N. M. Okun, J. C. Tarr, D. A. Hilleshiem, L. Zhang, K. I. Hardcastle and C. L. Hill, *J Mol Catal A: Chem*, 2006, **246**, 11-17.
37 N. M. Okun, T. M. Anderson and C. L. Hill, *J Am Chem Soc*, 2003, **125**, 3194-3195.
38 N. M. Okun, M. D. Ritorto, T. M. Anderson, R. P. Apkarian and C. L. Hill, *Chem Mater*, 2004, **16**, 2551-2558.
39 N. Okun, T. M. Anderson *and* C. L. Hill, *J Mol Catal A: Chem*, 2003, **197**, 283-290.
40 B. M. Smith, *Chem Soc Rev*, 2008, **37**, 470-478.
41 A. Sharma, A. Saxena, B. Singh, M. Sharma, M. V. Suryanarayana, R. P. Semwal, K. Ganeshan and K. Sekhar, *J Hazard Mater*, 2006, **133**, 106-112.
42 F. Liu, Q. F. Lu, X. L. Jiao and D. R. Chen, *Rsc Adv*, 2014, **4**, 41271–41276.
43 C. T. Buru, P. Li, B. L. Mehdi, A. Dohnalkova, A. E. Platero-Prats, N. D. Browning, K. W. Chapman, J. T. Hupp and O. K. Farha, *Chem Mater*, 2017, **29**, 5174-5181.
44 B. Singh, A. Saxena, A. K. Nigam, K. Ganesan and P. Pandey, *J Hazard Mater*, 2009, **161**, 933-940.
45 A. Saxena, B. Singh, A. K. Srivastava, M. V. S. Suryanarayana, K. Ganesan, R. Vijayaraghavan and K. K. Dwivedi, *Micropor Mesopor Mater*, 2008, **115**, 364-375.
46 M. T. Naseri, M. Sarabadani, D. Ashrafi, H. Saeidian and M. Babri, *Environ Sci Pollut Res*, 2013, **20**, 907-916.
47 M. Q. Zhao, Q. Zhang, J. Q. Huang and F. Wei, *Adv Funct Mater*, 2012, **22**, 675-694.
48 T. Kwon, G. A. Tsigdinos and T. J. Pinnavaia, *J Am Chem Soc*, 1988, **110**, 3654-3656.
49 Y. Chen, D. G. Yan and Y. F. Song, *Dalton Trans*, 2014, **43**, 14570-14576.
50 F. L. Yu and Y. Lu, *Appl Mech Mater*, 2014, **672-674**, 613-618.
51 P. Liu, C. H. Wang and C. Li, *J Catal*, 2009, **262**, 159-168.
52 Y. Watanabe, K. Yamamoto and T. Tatsumi, *J Mol Catal A: Chem*, 1999, **145**, 281-289.
53 E. Gardner and T. J. Pinnavaia, *Appl Catal A: Gen*, 1998, **167**, 65-74.
54 Y. Y. Liu, K. Murata, T. Hanaoka, M. Inaba and K. Sakanishi, *J Catal*, 2007, **248**, 277-287.
55 J. Das and K. M. Parida, *J Mol Catal A: Chem*, 2007, **264**, 248-254.
56 B. R. Jermy and A. Pandurangan, *J Mol Catal A: Chem*, 2005, **237**, 146-154.
57 Y. Wu, X. Y. Liu, Y. Q. Lei, Y. Qiu, M. L. Wang and H. Wang, *Appl Clay Sci*, 2017, **150**, 34-41.
58 T. F. Li, W. Zhang, W. Chen, H. N. Miras and Y. F. Song, ChemCatChem 2018, **10**, 188-197.
59 Y. Q. Xu, W. M. Xuan, M. M. Zhang, H. N. Miras and Y. F. Song, *Dalton Trans*, 2016, **45**, 19511-19518.

View Article Online
DOI: 10.1039/C9DT00395A

60 T. F. Li, H. N. Miras and Y. F. Song, *Catal*, 2017, **7**, 260.
61 J. Dong, H. J. Lv, X. R. Sun, Y. Wang, Y. M. Ni, B. Zou, N. Zhang, A. X. Yin, Y. N. Chi and C. W. Hu, *Chem Eur J*, 2018, **24**, 19208-19215.
62 C. M. Tourne, G. F. Tourne, S. A. Malik and T. J. R. Weakley, *J Inorg Nucl Chem* 1970, **32**, 3875-3890.
63 J. L. Gunjakar, T. W. Kim, H. N. Kim, I. Y. Kim and S. J. Hwang, *J Am Chem Soc*, 2011, **133**, 14998-15007.
64 L. S. Nogueira, S. Ribeiro, C. M. Granadeiro, E. Pereira, G. Feio, L. Cunha-Silva and S. S. Balula, *Dalton Trans*, 2014, **43**, 9518-9528.
65 T. A. G. Duarte, I. C. M. S. Santos, M. M. Q. Simoes, M. G. P. M. S. Neves, A. M. V. Cavaleiro and J. A. S. Cavaleiro, *Catal Lett*, 2014, **144**, 104-111.
66 T. A. G. Duarte, A. C. Estrada, M. M. Q. Simoes, I. C. M. S. Santos, A. M. V. Cavaleiro, M. G. P. M. S. Neves and J. A. S. Cavaleiro, *Catal Sci Technol*, 2015, **5**, 351-363.